ACS APPLIED MATERIALS & INTERFACES

Research Article

www.acsami.org

Gold-Nanorod-Based Colorimetric and Fluorescent Approach for Sensitive and Specific Assay of Disease-Related Gene and Mutation

Wenhong Wang, Yina Zhao, and Yan Jin*

Key Laboratory of Applied Surface and Colloid Chemistry, Ministry of Education, Key Laboratory of Analytical Chemistry for Life Science of Shaanxi Province, School of Chemistry and Chemical Engineering, Shaanxi Normal University, Xi'an 710062, China

Supporting Information

ABSTRACT: Sensitive and specific detection of disease-related gene and single nucleotide polymorphism (SNP) is of great importance in cancer diagnosis. Here, a colorimetric and fluorescent approach is described for detection of the p53 gene and SNP in homogeneous solution by using gold nanorods (GNRs) as both colorimetric probe and fluorescence quencher. Hairpin oligonucleotide was utilized as DNA probe to ensure highly sequence-specific detection of target DNA. In the presence of target DNA, the formation of DNA duplex greatly changed the electrostatic interaction between GNR and DNAs, leading to an obvious change in fluorescence and colorimetric response. The detection limit of fluorescent and colorimetric assay is 0.26 pM and 0.3 nM, respectively. Both fluorescence and colorimetric strategies were able to effectively discriminate complementary DNA from single-base mismatched DNA, which is meaningful for cancer diagnosis. More important, target DNA can be detected as low as 10 nM by the naked eye. Furthermore, transmission electron microscopy and fluorescence anisotropy measurements demonstrated that the color change as well as fluorescence quenching is ascribed to the DNA hybridization-induced aggregation of GNRs. Therefore, the assay provided a fast, sensitive, cost-effective, and specific sensing platform for detecting disease-related gene and SNP.

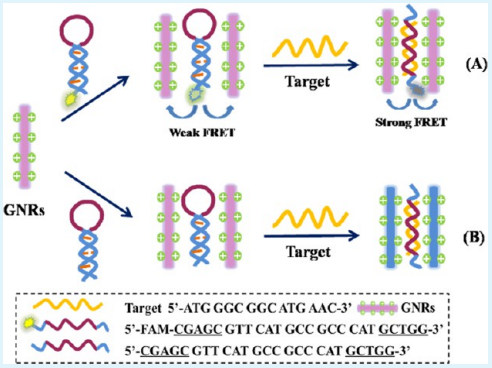

KEYWORDS: *hairpin DNA, gold nanorods, colorimetric assay, fluorescence, gene mutation*

1. INTRODUCTION

Sequence-specific DNA detection and single nucleotide polymorphism (SNP) play a significant role in areas including clinical and diagnostics studies, control of food safety, forensics, environmental monitoring, and so forth.[1−5] SNP mainly refers to the variation of single nucleotide within the DNA sequence. Some of these variations have been discovered to be directly linked to various human diseases.[6] For example, the p53 gene plays an important role in cell cycle control and apoptosis. Mutation of the p53 gene can be found in almost 50% of all human tumors.[7,8] By far, SNPs are found to be involved in the etiology of many human diseases, resulting in an increase in the development of diverse methods for SNP genotyping. Therefore, it is of significant importance to develop effective methods for detection of disease-related genes and SNP. As one of the promising probes for quantitative genomic studies, the molecular beacon (MB) is a hairpin-shaped oligonucleotide that can specifically report the presence of specific DNA, RNA, and protein in homogeneous solutions.[9,10] MB has significant potential for sequence-specific DNA detection and SNP assay due to its stem-loop structure. In general, conventional MBs are dually labeled with a fluorescence donor and fluorescence acceptor at the ends respectively, which leads to a complex synthesis and high cost. To overcome those disadvantages, there has been considerable interest in developing cost-effective detection of DNA in homogeneous solution by utilizing single-labeled hairpin DNA (hpDNA) as a recognition probe.[11−14] Yang et al. proposed a novel self-assembled MB/SWNT system for nucleic acid studies by using single-labeled hpDNA as the recognition probe and single walled nanotubes (SWNT) as the fluorescence quencher.[13] Lately, using single-labeled hpDNA as the recognition probe, Yang's and Fan's groups used GO as the nanoquencher for specific DNA detection.[15,16] Despite some progress, there still exist some problems regarding the sensitivity, response time, complex preparation, and treatment of SWNT and GO. To develop cost-effective and more universal methods, gold-nanorod-based colorimetric and fluorescent methods have been proposed for simple and rapid detection of p53 and SNP.

Gold nanomaterial, including gold nanoparticles and gold nanorods, is a type of promising nanomaterial and plays important roles in biosensing and bioanalysis due to its unique optical properties and good biocompatibility. Owing to its anisotropic rod-shape, gold nanorods have offered diverse potentials for biomedical and bioanalytical applications, such as the studies of biochemical reaction, nucleic acids, metal ions, amino acids, and protein.[17−24] Herein, we established a colorimetric and fluorescent method for the detection of p53

Received: August 16, 2013
Accepted: October 23, 2013
Published: October 23, 2013

gene and SNP based on target−induced changes in electrostatic interactions between DNA and GNRs. The changes in absorbance and fluorescence were utilized to highly sensitive study the sequence-specific molecular recognition. Taking advantage of the high target-specificity of hpDNA, fully complementary DNA can be distinguished from single-base mismatch DNA. So, it successfully explored the potential application of gold nanorods in developing a universal, cost-effective, and reliable biosensing platform.

2. EXPERIMENTAL SECTION

Chemicals. All oligonucleotides were synthesized by Sangon Biotech Co. (Shanghai, China). Chloroauric acid ($HAuCl_4{\cdot}4H_2O$), sodium borohydride ($NaBH_4$), ascorbic acid, and cetyltrimethylammonium bromide(CTAB) were purchased from Beijing Dingguo Biotechnology Co., Ltd. (Beijing, China). All of the metal salt was purchased from Xi'an chemical reagent Co., Ltd. (Xi'an, China). Tris-HCl buffer (20 mM, pH = 7.5) was used to prepare the oligonucleotides stock solutions.

Instrumentation. All fluorescence measurements were performed on a Hitachi F-7000 fluorescence spectrophotometer (Tokyo, Japan). UV−visible absorption spectra were recorded on a Hitachi U-3900H UV/Vis spectrophotometer (Tokyo, Japan). Transmission electron microscopy (TEM) images were collected on a JEM-2100 instrument (Jeol Co. Ltd, Tokyo, Japan).

Synthesis of Gold Nanorods (GNRs). Gold nanorods were synthesized by chemical reduction process using a seeding growth method according to the literature.[25,26] The synthesis process has been briefly described in the previous work.[17] The properties of prepared GNRs were characterized by TEM and UV−vis absorption spectrum measurements.

Fluorescence Experiments. The changes in fluorescence spectra were recorded on a fluorometer (F-7000, Hitachi). The fluorescence in the range of 500−600 nm was measured with excitation at 480 nm. First, the fluorescence of 100 μL of 20 nM F-hpDNA was read. Then, 0.5 μL of GNRs was added and incubated for 5 min before fluorescence measurements. Subsequently, target DNAs were added. DNA hybridization was carried out in Tris-HCl buffer (20 mM Tris-HCl, 100 mM NaCl, pH = 7.5) for 5 min.

Fluorescence Polarization Measurements. The detail of fluorescence polarization measurements was just as mentioned in the previous work.[17] The equation of fluorescence polarization (P) was as follows:[27]

$$P = \frac{I_{\parallel} - I_{\perp}}{I_{\parallel} + I_{\perp}}$$

$I_{\parallel}$ and $I_{\perp}$ are the vertically and horizontally polarized emission, respectively, excited by vertically polarized light. Changes in fluorescence anisotropy were recorded within 5 min.

UV Measurements. First, the UV−vis absorption spectra of 1.45 nM GNRs were read in the range of 400−900 nm. Then, hpDNA was added and incubated for 10 min. Subsequently, target DNAs with different concentration were added and incubated for 10 min.

3. RESULTS AND DISCUSSION

Proof of Principle. As depicted in Figure 1, GNRs-based FRET and colorimetric assay have been proposed to detect the p53 gene and SNP using gold nanorods as the fluorescence quencher and colorimetric probe, respectively. Carboxyfluorescein-tagged hairpin DNA (F-hpDNA) was used as a DNA probe for fluorescence assay. The CTAB-coated GNR is positively charged. When hpDNA or F-hpDNA is mixed with GNRs, the electrostatic interaction between GNRs and DNA probe attracted DNA close to the surface of GNRs, leading to a decrease in longitudinal absorption of GNRs and fluorescence quenching of F-hpDNA. DNA hybrid is formed when input

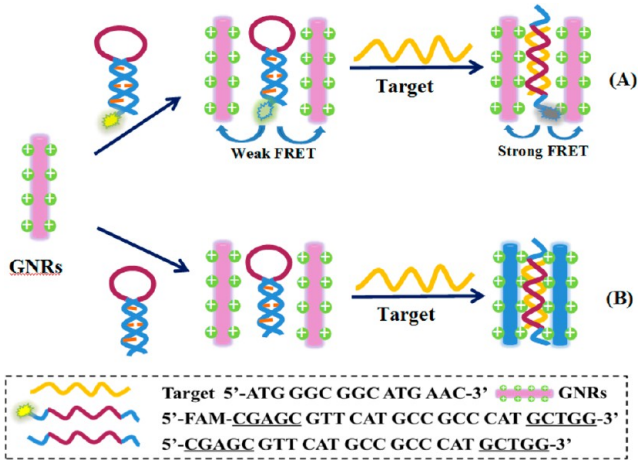

Figure 1. Schematic description of the GNRs-based fluorescent (A) and colorimetric (B) strategy for detection of DNA and SNP.

target DNA, which strengthened the electrostatic interaction between GNRs and DNA and led to the aggregation of GNRs. As a result, the longitudinal absorption of GNRs obviously decreased and the fluorescence of F-hpDNA was further quenched. So, target DNA can be specifically detected by colorimetric and fluorescence approach.

To verify the feasibility of fluorescence protocol, the fluorescence response of F-hpDNA under different conditions was investigated. It can be clearly found from Figure 2 that the

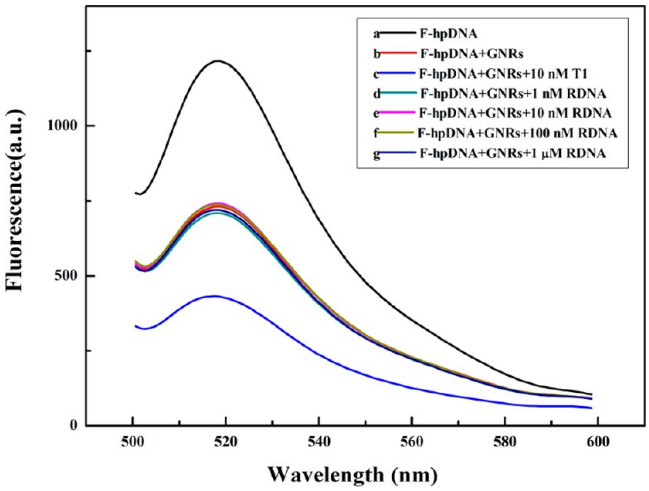

Figure 2. Fluorescence spectra of F-hpDNA under different conditions. (a) F-hpDNA, (b) a + GNRs, (c) b +10 nM T1, and (d−g) F-hpDNA/GNRs with RDNA from 0.001 to1 μM.

input of GNRs induced a decrease (~ 46%) in the fluorescence intensity of F-hpDNA (curve b), indicating that FRET occurred between F-hpDNA and GNRs. Upon the addition of T1, fluorescence of the F-hpDNA/GNRs mixture further decreased. This fact can be ascribed to the formation of DNA hybrids that have higher surface charge than ssDNA. Therefore, the electrostatic interaction between GNRs and F-hpDNA/T1 hybrid enhanced, leading to an increase in the FRET efficiency. To exclude other possibilities of false signal, negative control experiments have been designed. First, the fluorescence response of F-hpDNA/GNRs mixture in the presence of random DNA was studied. Figure 2 demonstrated that random

DNA strand has no effect on the fluorescence of F-hpDNA/GNRs mixture. Secondly, the influence of reaction time on the fluorescence was studied. Figure S1A in the Supporting Information demonstrates that the fluorescence of the F-hpDNA and F-hpDNA/GNRs mixtures slightly changed as time goes on. Therefore, the fluorescence quenching was not attributed to the bleaching of dye with elapsing time. Finally, the effect of T1 on the fluorescence intensity of F-hpDNA was studied. Figure S1B reveals that the fluorescence of F-hpDNA cannot be quenched by T1 in the absence of GNRs. Based on the above results, we draw a conclusion that fluorescence quenching is ascribed to the specific molecular recognition between DNA probe and target, and GNRs-based FRET for DNA detection is feasible and reasonable.

Colorimetric assay (Figure 1B) utilizes the fact that changes in electrostatic interaction between GNRS and DNAs will affect the properties of GNRs. The UV−vis absorbance spectra of GNRs in Figure 3 display a transverse absorption peak around

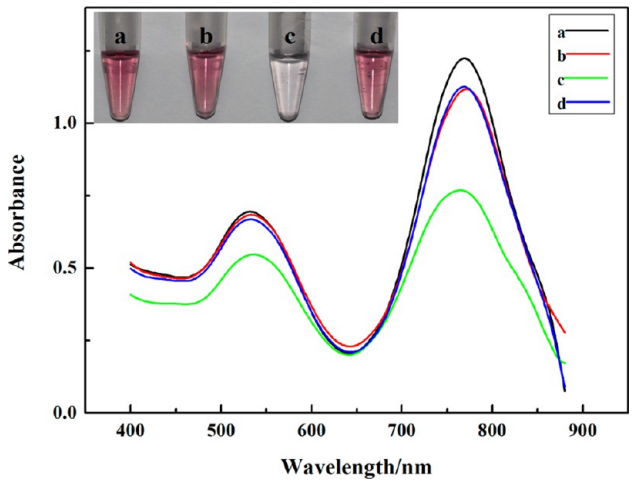

Figure 3. Absorbance spectra of GNRs under different conditions. (a) GNRs, (b) GNRs/20 nM hpDNA, (c) b+50 nM T1, and (d) b+50 nM random DNA. Inset photographic images are the corresponding colorimetric response.

530 nm and a longitudinal absorption peak around 770 nm (curve a). When hpDNA is mixed with GNRs suspension, the UV−vis absorption spectra of GNRs slightly changed (curve b). Since the negative charge density of ssDNA is much lower than that of dsDNA. So, the electrostatic interactions between ssDNA and GNRs just attracted DNA close the surface of GNRs, and could not induce an obvious change in state of GNRs. Upon addition of the T1 (curve c), a marked change in the UV−vis absorption spectra of GNRs occurred. The transverse absorption peak slight red shifted, while the intensity of longitudinal absorption distinctly decreased accompanying with a blue-shift. That is, DNA hybridization significantly changed the state of GNRs. The strengthened electrostatic interactions between GNRs and dsDNA caused the assembly of GNRs, leading to a significant decrease in the longitudinal absorption of GNRs. Therefore, changes in absorbance can be utilized for quantitative determination of target DNA. Moreover, change in the color of GNR can directly reflect the presence of target DNA. Curve d in Figure 3 demonstrates the colorimetric response of hpDNA/GNRs mixture in the presence of random DNA. As expected, there is no fundamental change compared with hpDNA/GNRs. All these results revealed that the change in color and absorbance of GNRs was attributed to the specific DNA hybridization. It further verified the feasibility of our colorimetric approach.

Optimization of Experimental Conditions. Since many factors may affect the sensing performance, the influences of these factors were investigated. First, the effect of reaction time on the fluorescence intensity of F-hpDNA should be considered. From Figure S1A it could be found that the fluorescence of F-hpDNA hardly changed as time goes on (Figure S1B). Meanwhile, the fluorescence intensity of both F-hpDNA/GNRs and F-hpDNA/GNRs/T1 reached a minimum in 5 min and almost remained constant after that. Secondly, the influence of pH in the range of 6.5−8.0 was studied. It is clear from Figure S2 that the FRET efficiency improved as the pH value increased in the range of 6.5−7.5. The biological process is highly related to pH; a small change in pH obviously affected the reaction rate of the biological process. So the DNA hybridization efficiency is high under the conditions similar to physiological status. Then the response decreased gradually once pH over 7.5. It may be attributed to the fact that higher pH is unfavorable for the DNA hybridization reaction. Therefore, pH 7.5 was chosen as the optimized condition. Thirdly, the effect of ionic strength on the quenching efficiency was studied. From information given in Figure S3, we discovered that the quenching efficiency improved significantly with the increase of NaCl concentration in the range of 0−0.1 mol L^{-1}. However, FRET efficiency decreased when the concentration of NaCl exceeded 0.1 mol L^{-1}. Under lower ionic strength, an increase in ionic strength may be helpful to DNA hybridization efficiency, resulting in a higher FRET efficiency. While the electrostatic interaction between DNA and GNRs reduced under high ionic strength. Meanwhile, greater than 100 mM of NaCl made the GNRs unstable.[28−33] So, the optimal concentration of NaCl is 0.10 mol L^{-1} for this study.

It has been reported that the location of absorption peak depends on the aspect ratio of GNRs.[17] In this study, four kinds of GNRs were prepared via adjusting the amounts of initial silver nitrate from 100 to 500 μL (Figure S4). According to the results of TEM, the average aspect ratio of GNRs was 1.8, 2.5, 3.5, and 3, respectively(Figure S5). As the aspect ratio of GNRs will affect the absorption peak, the effect of amount and aspect ratio of GNRs on the FRET efficiency should be investigated. It can be discovered from the Figure S6A that the optimal average aspect ratio of GNRs was 3.5 in this study. Moreover, the fluorescence quenching efficiency was appropriate when 0.5 μL of GNRs was used as the fluorescence quencher (Figure S6B).

Mechanism Investigation. To further verify the sensing mechanism, TEM imaging and fluorescence polarization were performed. Based on the TEM images in Figure 4A, it was observed that GNRs dispersed well without hpDNA. As shown in Figure 4B, the space of GNRs became smaller when hpDNA was mixed with GNRs. However, the formation of hpDNA/T1 hybrid led to the assembly of GNRs (image C). The TEM result is in good accordance with fluorescent and colorimetric measurements.

Furthermore, the sensing mechanism was further studied by the fluorescence polarization (FP) assay. Fluorescence polarization has been a valuable tool for biophysical research such as nucleic acid hybridization, protein−protein interaction, and interaction between biomolecules and small molecules.[34−36] Figure S7A demonstrates the fluorescence polarization (FP) of F-hpDNA probe under different conditions. The FP value of F-hpDNA is relatively low. An increase in FP value was obtained

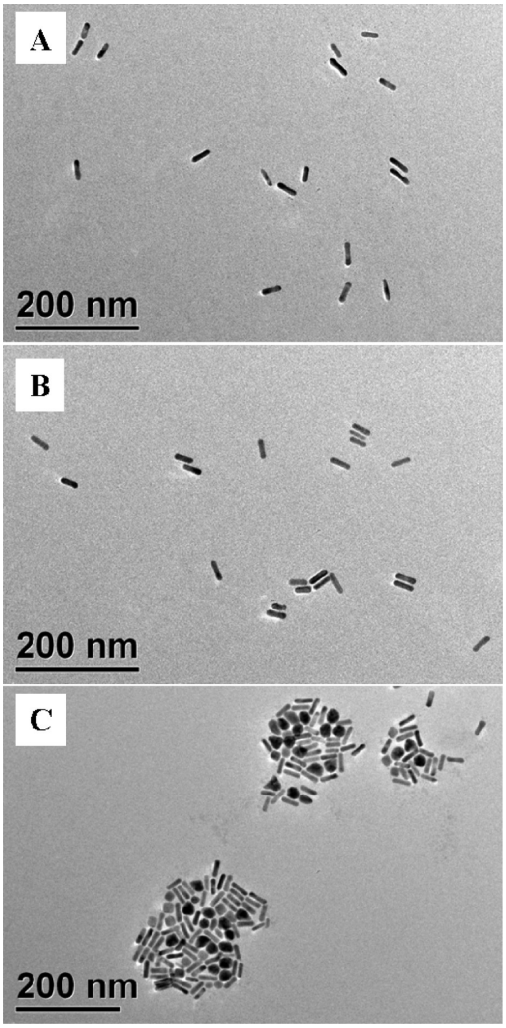

Figure 4. TEM images of (A) GNRs and GNRs in the presence of (B) hpDNA and (C) hpDNA/T1 hybrid.

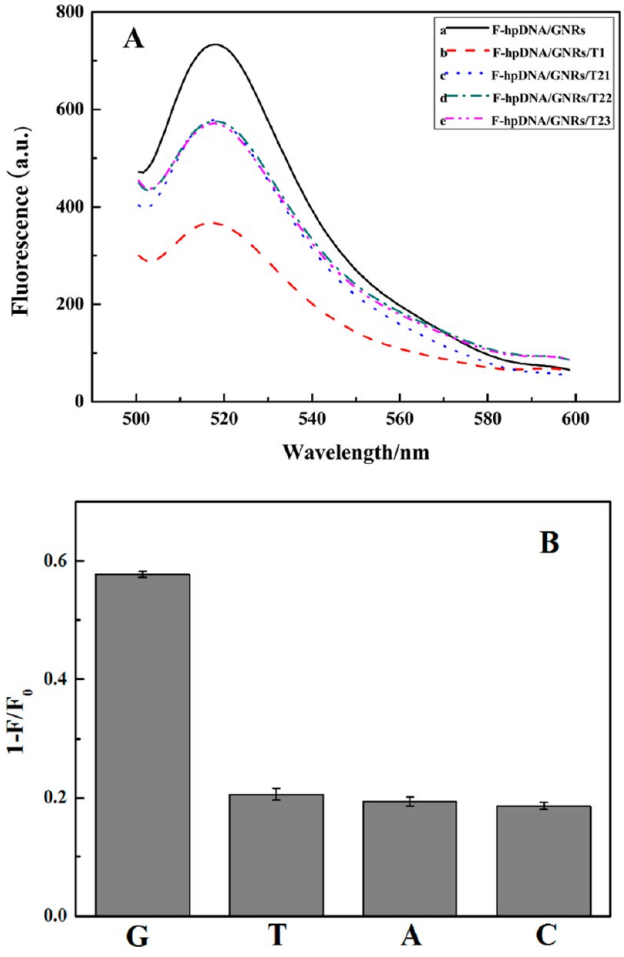

Figure 5. (A) Fluorescence spectra of F-hpDNA/GNRs in the presence of complementary (T1) and single-base mismatched DNAs. The mutation base of T21, T22, and T23 is T, A, and C, respectively. (B) Bar chart of fluorescence response of target DNAs to F-hpDNA/GNRs mixture. The error bar represents the standard deviation from three independent experiments, where F_0 and F are the F-hpDNA/GNRs intensities in the absence and presence of target DNA, respectively.

when F-hpDNA mixed with GNRs. However, the FP value of F-hpDNA/GNRs mixture greatly increased after addition of T1. Moreover, it gradually increased as the T1 concentration increased (Figure S7B). Such an increase in fluorescence polarization was attributed to the fact that the motion of the F-hpDNA has been confined due to the strong electrostatic interaction between dsDNA and GNRs. Therefore, fluorescence polarization and TEM measurements further proved the principle of our method.

Fluorescent and Colorimetric Detection of SNP. To investigate the ability to identify SNP, we firstly compared the FRET efficiency in the presence of T1 and single-base mutation DNAs. It is clear from Figure 5 that the proposed method has a remarkably high specificity to discriminate complementary target from single-base mismatched DNA. Then, we further investigated the recognition capability to detect target DNAs with different mutation numbers. The sequences of these mismatched DNAs are demonstrated in Table 1. As shown in Figure 6A, the FRET efficiency decreased proportionally with the increase in mutation number of DNA. Hairpin DNA has a stem-loop structure, which gives it higher specificity for mutation recognition. Single-base mismatched target DNA has much lower hybridization efficiency with hpDNA than that of complementary target DNA. Meanwhile, we tested the

Table 1. Summary of Oligonucleotide Sequences

oligonucleotide	sequence
F-hpDNA: FAM-labeled hairpin DNA	5′-FAM-**CGAGC**GTTCATGCCGCCCAT**GCTCG**-3′
hpDNA: hairpin DNA	5′ −**CGAGC**GTTCATGCCGCCCAT**GCTCG**-3′
T1: complementary target DNA	5′-ATGGGC**G**GCAT GAAC-3′
T21: single-base mismatch DNA	5′-ATGGGC**T**GCATGAAC-3′
T22: single-base mismatch DNA	5′-ATGGGC**A**GCATGAAC-3′
T23: single-base mismatch DNA	5′-ATGGGC**C**GCATGAAC-3′
T3: two-bases mismatch DNA	5′-ATGGG**A**GGC**C**TGAAC-3′
T4: three-bases mismatch DNA	5′-AT**T**GGC**T**GCATG**C**AC-3′
RDNA: random DNA	5′-ATATCATATTTGGTG-3′

dx.doi.org/10.1021/am4034119 | ACS Appl. Mater. Interfaces 2013, 5, 11741−11746

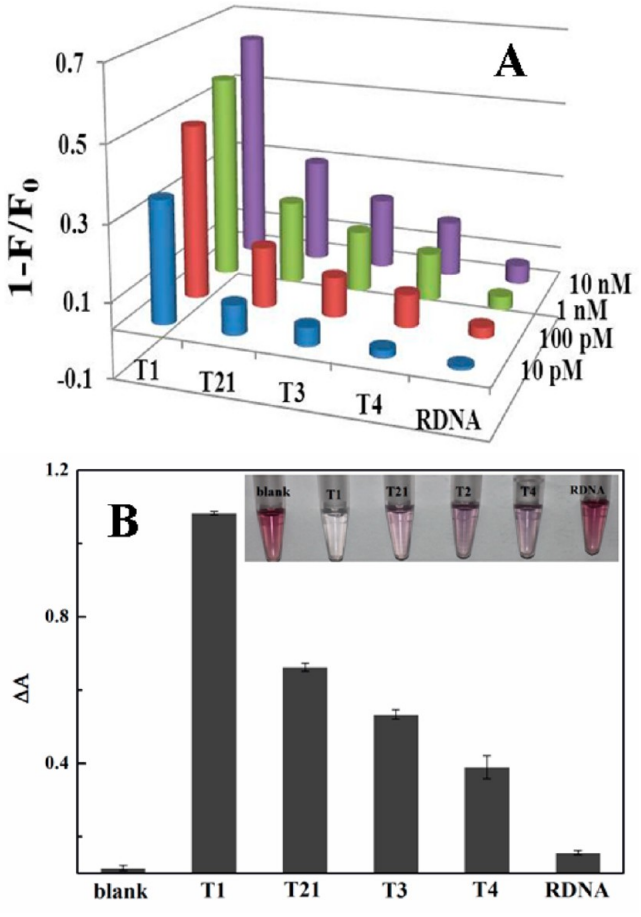

Figure 6. (A) Fluorescence response of F-hpDNA/GNRs in the buffer as the concentration of target DNAs increased from 10 pM to 10 nM. (B) Colorimetric response of hpDNA/GNRs in the buffer towards different DNAs. The concentration of all DNAs is 100 nM. Inset is the corresponding photographs.

specificity of colorimetric analysis. It is obvious from Figure 6B that SNP can be easily and sensitively discriminated from T1, as well as other mismatched DNA strands, by comparing the change of absorbance peak around 770 nm. As a result, complementary DNA can be sensitively and easily discriminated from mutation and random DNAs by the change in color of GNRs. These facts revealed that the GNRs-based colorimetric and fluorescent method could be used to sensitively and selectively discriminate SNP.

Sensitivity of Fluorescent and Colorimetric Detection of p53 Gene. To verify the potential application for quantitative analysis, the relationship between fluorescence response and target concentration has been studied. As expected, the change in fluorescence intensity is directly related to T1 concentration. The inset of Figure 7A demonstrates that there is a remarkable linear relationship between quenching efficiency and logarithmic concentrations of T1 in the range of 0.001−100 nM. The limit of detection was 0.26 pM, indicating that it is a highly sensitive method compared with previously reported fluorescence methods (Table S1).

Under the optimized conditions, target-induced changes in absorption spectra of GNRs were recorded. It was discovered in Figure 7B that the absorbance peaks of GNRs at both 530 nm and 770 nm gradually decreased with the increasing of amount of T1. Since the high sensitivity of the longitudinal plasmon

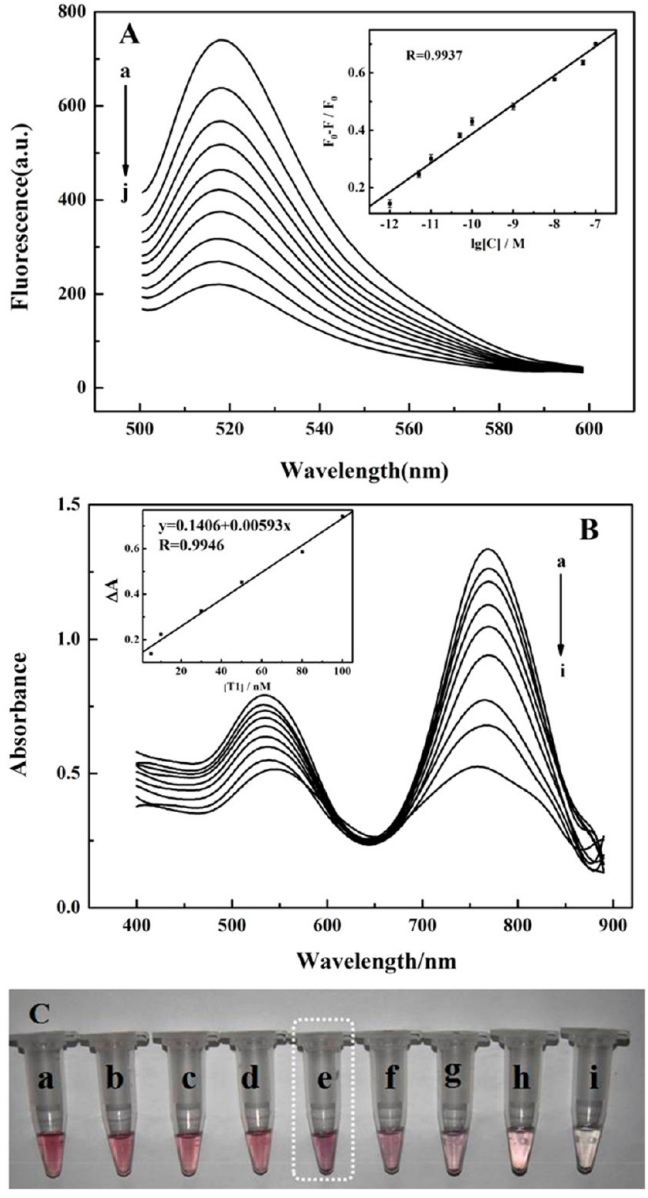

Figure 7. (A) Fluorescence spectra of F-hpDNA/GNRs in the absence/presence of different concentrations of T1. From curve (a) to (j), the concentration of T1 is 0, 0.001, 0.005, 0.01, 0.05, 0.1, 1, 10, 50, and 100 nM, respectively. (Inset) Linear correlation of the fluorescence change versus logarithmic concentrations of T1. (B) UV−vis absorption of GNRs in the absence and presence of DNA. (a) GNRs, (b−i) GNRs/hpDNA + T1; from (b) to (i), the concentration of T1 is 0, 1, 5, 10, 30, 50, 80, and 100 nM, respectively. (Inset) Linear correlation of the absorbance change versus the concentrations of T1. (C) Color changes of GNRs for visual detection of T1.

band to the interparticle interaction[27,37,38] compared with the transversal absorption band, a obvious change in intensity of longitudinal absorbance band was utilized to quantitatively analyze target DNA. A good linear correlation between absorbance difference and T1 concentration in the range of 5−100 nM was obtained. GNRs-based colorimetric method is sensitive with a detection limit of 0.3 nM (Figure 7B). Meanwhile, it has been observed that the longitudinal absorption peak blue shifted upon addition of target DNA, accompanying a smaller red-shift of the transverse band. The change in color of GNRs has also been observed (Figure 7C).

Based on that, T1 can be sensitively detected as low as 10 nM by the naked eye. These above results further proved that our method is simple and sensitive compared with most other methods (Table S1).

4. CONCLUSIONS

In summary, a GNRs-based colorimetric and fluorescent approach for DNA detection and SNP discrimination has been developed. In comparison with previous reports, this assay presents the following unique features. Firstly, by utilizing GNRs as the colorimetric probe, the p53 gene can be simply and sensitively detected at as low as 0.3 nM by the change in absorbance and at 10 nM by the naked eye without external labeling. Secondly, hairpin DNA probe is single-labeled for the fluorescent assay by using GNRs as the fluorescence quencher, which exhibited some excellent features, including relative ease of synthesis, high stability, and low cost. Thirdly, based on the inherent specificity of the hairpin DNA, complementary DNA was sensitively distinguished from single-base mismatched DNAs and random DNA by the change in fluorescence intensity, and absorbance or color of GNRs solution. Moreover, GNRs-based fluorescent method can sensitively detect target DNA at as low as 0.26 pM. Therefore, this assay provided a fast and more universal method for the assay of disease-related DNA and SNP in homogeneous solution with high selectivity and sensitivity, and will find potential applications in genetic studies and disease diagnosis.

■ ASSOCIATED CONTENT

Supporting Information

Fluorescence intensity of F-hpDNA under different conditions, effect of pH and ionic strength on the FRET efficiency, photographic images of GNRs, UV−vis absorption spectrum of GNRs with different aspect ratios, influence of aspect ratio (A) and amount (B) of gold nanorods on the FRET efficiency, change in fluorescence polarization, and comparison of different methods for DNA detection. This material is available free of charge via the Internet at http://pubs.acs.org.

■ AUTHOR INFORMATION

Corresponding Author

*Tel: 86-29-81530726. Fax: 86-29-81530727. E-mail: jinyan@snnu.edu.cn.

Notes

The authors declare no competing financial interest.

■ ACKNOWLEDGMENTS

This work was financially supported by the National Natural Science Foundation of China (No. 21075079), Program for New Century Excellent Talents in University (No. NCET-10-0557), and the Program for Cangjiang Scholars and Innovative Research Team in University (IRT 1070). This project was funded by Hunan University.

■ REFERENCES

(1) Lanciotti, R. S.; Kerst, A. J. *J. Clin. Microbiol.* **2001**, *39*, 4506−4513.
(2) Monis, P. T.; Giglio, S. *Infect., Genet. Evol.* **2006**, *6*, 2−12.
(3) Jonas, D. A.; Elmadfa, I.; Engel, K. -H.; Heller, K J.; Kozianowski, G.; König, A.; Müller, D.; Narbonne, J. F.; Wackernagel, W.; Kleiner, J. *Ann. Nutr. Metab.* **2001**, *45*, 235−254.
(4) Alford, R. L.; Caskey, C. T. *Curr. Opin. Chem. Biol.* **1994**, *5*, 29−33.
(5) Palchetti, I.; Mascini, M. *Analyst* **2008**, *133*, 846−854.
(6) Collins, A.; Lonjou, C.; Morton, N. E. *Proc. Natl. Acad. Sci. U.S.A.* **1999**, *96*, 15173−15177.
(7) Nakano, K.; Vousden, K. H. *Mol. Cell* **2001**, *7*, 683−694.
(8) Ye, S.; Dhillon, S.; Ke, X.; Collins, A. R.; Day, I. N. M. *Nucleic Acids Res.* **2001**, *29*, e88.
(9) Hwang, G. T.; Seo, Y. J.; Kim, B. H. *J. Am. Chem. Soc.* **2004**, *126*, 6528−6529.
(10) Tyagi, S.; Kramer, F. R. *Nat. Biotechnol.* **1996**, *14*, 303−308.
(11) Dong, H.; Gao, W.; Yan, F.; Ji, H.; Ju, H. *Anal. Chem.* **2010**, *82*, 5511−5517.
(12) Zhang, Y.; Tang, Z.; Wang, J.; Wu, H.; Maham, A.; Lin, Y. *Anal. Chem.* **2010**, *82*, 6440−6446.
(13) Yang, R.; Jin, J.; Chen, Y.; Shao, N.; Kang, H.; Xiao, Z.; Tang, Z.; Wu, Y.; Zhu, Z.; Tan, W. *J. Am. Chem. Soc.* **2008**, *130*, 8351−8358.
(14) Kim, Y. S.; Kim, B. C.; Lee, J. H.; Kim, J.; Gu, M. B. *Biotechnol. Bioprocess Eng.* **2006**, *11*, 449−454.
(15) Lu, C.-H.; Li, J.; Liu, J.-J.; Yang, H.-H.; Chen, X.; Chen, G.-N. *Chem.—Eur. J.* **2010**, *16*, 4889−4894.
(16) Li, F.; Huang, Y.; Yang, Q.; Zhong, Z.; Li, D.; Wang, L. *Nanoscale* **2010**, *2*, 1021−1026.
(17) Deng, J.; Jin, Y.; Wang, L.; Chen, G.; Zhang, C. *Biosens. Bioelectron.* **2012**, *34*, 144−150.
(18) He, W.; Huang, C. Z.; Li, Y. F.; Xie, J.P.; Yang, R. G.; Zhou, P. F.; Wang, J. *Anal. Chem.* **2008**, *80*, 8424−8430.
(19) Dujardin, E.; Hsin, L.-B.; Wang, C. R. C.; Mann, S. *Chem. Commun.* **2001**, *14*, 1264−1265.
(20) Chen, G.; Jin, Y.; Wang, L.; Deng, J.; Zhang, C. *Chem. Commun.* **2011**, *47*, 12500−12502.
(21) Wang, L.; Jin, Y.; Deng, J.; Chen, G. *Analyst* **2011**, *136*, 5169−5174.
(22) Sudeep, P. K.; Joseph, S. T. S.; Thomas, K. G. *J. Am. Chem. Soc.* **2005**, *127*, 6516−6517.
(23) Yu, C.; Irudayaraj, J. *Anal. Chem.* **2007**, *79*, 572−579.
(24) Wang, J.; Zhang, P.; Li, J. Y.; Chen, L. Q.; Huang, C. Z.; Li, Y. F. *Analyst* **2010**, *135*, 2826−2831.
(25) Nikoobakht, B.; El-Sayed, M. A. *Chem. Mater.* **2003**, *15*, 1957−1962.
(26) Sau, T. K.; Murphy, C. J. *Langmuir* **2004**, *20*, 6414−6420.
(27) Huang, Y.; Chen, J.; Shi, M.; Zhao, S.; Chen, Z. F.; Liang, H. *J. Mater. Chem. B* **2013**, *1*, 2018−2021.
(28) Liu, J.; Wang, H.; Yan, X. *Analyst* **2011**, *136*, 3904−3910.
(29) Lu, X.; Dong, X.; Zhang, K.; Han, X.; Fang, X.; Zhang, Y. *Analyst* **2013**, *138*, 642−650.
(30) Deng, J.; Jin, Y.; Wang, L.; Chen, G.; Zhang, C. *Biosens. Bioelectron.* **2012**, *34*, 144−150.
(31) He, W.; Huang, C.; Li, Y.; Xie, J.; Yang, R.; Zhou, P.; Wang, J. *Anal. Chem.* **2008**, *80*, 8424−8430.
(32) Leal, C.; Moniri, E.; Pegado, L.; Wennerstrom, H.. *J. Phys. Chem. B* **2007**, *111*, 5999−6005.
(33) Ganachaud, F.; Elaıssari, A.; Pichot, C. *Langmuir* **1997**, *13*, 7021−7029.
(34) Kumke, M. U.; Shu, L.; McGown, L. B. *Anal. Chem.* **1997**, *69*, 500−506.
(35) Zhang, M.; Guan, Y.-M.; Ye, B.-C. *Chem. Commun.* **2011**, *47*, 3478−3480.
(36) Lea, W. A.; Simeonov, A. *Expert Opin. Drug Discovery* **2011**, *6*, 17−32.
(37) Fu, X.; Chen, L.; Li, J.; Lin, M.; You, H.; Wang, W. *Biosens. Bioelectron.* **2012**, *34*, 227−231.
(38) Pramod, P.; Thomas, K. G. *Adv. Mater.* **2008**, *20*, 4300−4305.